

## Single Crystal Manganese Oxide Multipods by Oriented Attachment

David Zitoun,<sup>\*,†</sup> Nicola Pinna,<sup>‡,§</sup> Nathalie Frolet,<sup>†</sup> and Claude Belin<sup>†</sup>

Laboratoire des Agrégats Moléculaires et Matériaux Inorganiques, UMR 5072 CC15, Université Montpellier II, Place Eugène Bataillon, 34095 Montpellier, France, Institut für Anorganische Chemie, Martin-Luther-Universität Halle-Wittenberg, Kurt-Mothes-Str. 2, 06120 Halle (Saale), Germany, and Max-Planck-Institute of Microstructure Physics, Weinberg 2, D-06120 Halle, Germany

Received August 16, 2005; E-mail: zitoun@univ-montp2.fr

Chemical synthesis has produced nice examples of well-defined nanocrystals (NCs).<sup>1</sup> Semiconducting NCs have been the object of great interest and solution synthesis leading to a variety of shapes, including rods,<sup>2</sup> tetrapods,<sup>3</sup> prisms,<sup>4</sup> cubes,<sup>5</sup> and additional shapes.<sup>6</sup> In the case of tetrapods, the synthesis involves a two-step mechanism, which clearly separates nucleation from growth. Tetrapods crystallized as regular tetrahedra from both gas phase<sup>7</sup> and solution phase synthesis.<sup>2</sup> This approach was a first step to the architectural control at the nanoscale as has already been observed on the molecular scale. Shape control was achieved mainly for a material which presents an anisotropic crystal structure, for instance, a hexagonal compact lattice. A second step would be the shape control for any highly symmetric crystal structure, as already explored for noble metals such as silver,<sup>8</sup> gold,<sup>9</sup> or platinum.<sup>10</sup>

In this communication, we report the single-step synthesis of manganese oxide (MnO) single-crystalline multipods. The unique characteristics of transition metal oxides make them the most diverse class of materials, with properties covering almost all aspects of materials science and solid state physics.<sup>11</sup> MnO is considered as a model for the understanding of magnetic properties.<sup>12</sup> MnO displays an antiferromagnetic–ferromagnetic transition for clusters, and Mn<sup>2+</sup> is a spin only transition metal.

Nowadays, nonhydrolytic sol–gel processes in organic solvents have become very popular for the synthesis of metal oxide NCs.<sup>13</sup> The synthesis is based on the thermal decomposition of Mn(oleate)<sub>2</sub> in *n*-trioctylamine. In the presence of oleic acid, the synthesis yields almost exclusively hexapods that are very homogeneous in size and shape. All reactants, products, and byproducts are environmentally friendly and very stable in air. This approach<sup>14</sup> was recently used to synthesize high quality oxide NCs with narrow size dispersion and without any size-selective precipitation.<sup>15–17</sup>

In a typical synthesis, 5 mmol of Mn(oleate)<sub>2</sub> (synthesized according to published methods)<sup>16</sup> and 0.5 equiv of oleic acid (Aldrich) were dissolved in 30 mL of trioctylamine (Fluka) by stirring at 90 °C for 15 min. The solution was then quickly heated to 320 °C over 20 min and maintained at high temperature for 30 min. The orange solution turned light green. The solution was then cooled to room temperature without stirring. The brown solution was precipitated with ethanol, and a brown powder was isolated from centrifugation. The reaction yielded NCs redispersed in cyclohexane.

The NCs were characterized using transmission electron microscopy (TEM, JEOL 4010 operating at 400 kV or Philips CM20 operating at 200 kV), X-ray powder diffraction (XRD, Philips analytical X'pert), and a SQUID magnetometer (Quantum Design MPMS XL) (see Supporting Information, Figures 4 and 5). TEM

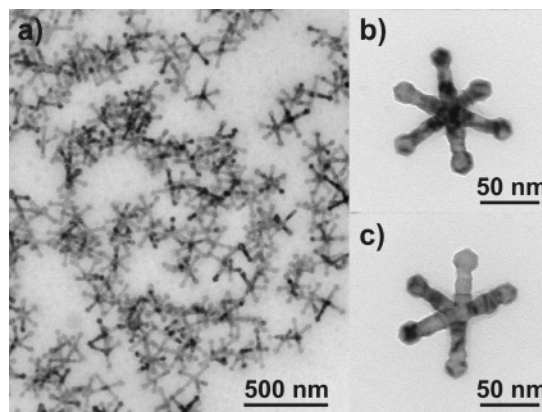


**Figure 1.** Overview TEM image of an assembly of MnO multipods (a), a hexapod (b), and a pentapod (c).

samples were prepared by placing a drop of a dilute cyclohexane dispersion of NCs. XRD and SQUID measurements were performed on a powder dried at room temperature. The experimental XRD pattern exhibited a series of Bragg reflections corresponding to the standard cubic rock salt of manganosite ( $Fm\bar{3}m$ ,  $a = 4.445 \text{ \AA}$ ). The NCs were found to be phase pure and highly crystalline.

The material displayed an antiferromagnetic behavior with a Néel temperature ( $T_N = 125 \text{ K}$ ) close to the bulk value ( $T_N = 118 \text{ K}$ ). Above this temperature, the susceptibility followed a classical Curie–Weiss law. The magnetic measurements were then found to be in very good agreement with the experimental studies; size and shape effects were not noticeable. Size effect was only observed for smaller nanocrystals which exhibited a superparamagnetic behavior.<sup>18</sup> Contrary to spherical particles up to 25 nm, the multipods exhibit a magnetic behavior similar to that of the bulk despite the size of the arms.<sup>17</sup>

TEM study showed very homogeneous NCs around 200 nm in size (Figure 1). Most of the multipods appeared to be hexapods with an  $O_h$  symmetry even if some of the NCs displayed only 2, 3, 4, or 5 pods. All of the NCs were single-crystalline as evidenced by electron diffraction and high resolution study. Cores and pods were found to be homogeneous in size and morphology, each arm being terminated by an arrow.

Selected area electron diffraction (SAED) measured from isolated multipods showed patterns similar to the one presented in Figure 2b. The SAED showed sharp single spots characteristic of a monocrystal of MnO (manganosite) oriented along the [001] direction with its arms parallel to the [100] and [010] directions, respectively. These findings were further proved by high-resolution transmission electron microscopy (HRTEM). The image of the end of an arm (Figure 2c) showed well-defined lattice planes, a magnification of the white squared zone, and its power spectrum

<sup>†</sup> Université Montpellier II.

<sup>‡</sup> Martin-Luther-Universität Halle-Wittenberg.

<sup>§</sup> Max-Planck-Institute of Microstructure Physics.

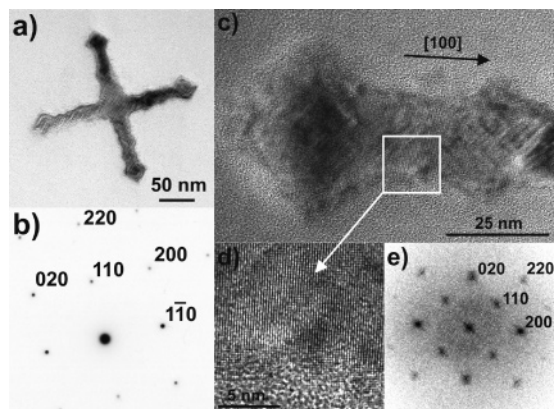


**Figure 2.** TEM image of a single tetrapod (a), SAED (b), HRTEM of a single arm (c), the magnification of the white square (d), and its square of the Fourier transform (power spectrum) (e).

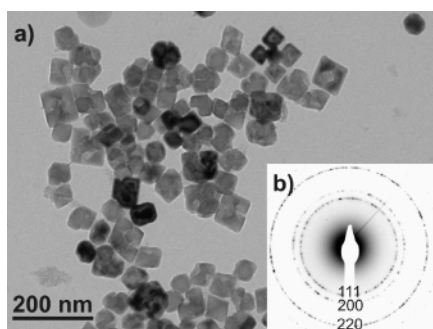


**Figure 3.** Overview TEM image of the nanocrystals grown for 30 min only (a) and its related electron diffraction (ED) (b).

(i.e., square of the Fourier transform) (Figure 2d and e) confirmed the good crystallinity of the multipods and their growth orientation.

The anisotropy of crystal structure or crystal surface reactivity was identified in the literature as the main driving force for the growth of anisotropic nanostructures. However, 1-D growth of MnO rocksalt NCs with their symmetric cubic lattice is rather unexpected. A close look to the pods reveals a zigzag growth already observed for the oriented attachment mechanism. This growth mechanism as evidenced in other oxides, such as  $\text{TiO}_2$ ,<sup>19</sup>  $\text{ZnO}$ ,<sup>20</sup> or cubic chalcogenides such as  $\text{CdTe}$ <sup>21</sup> and  $\text{PbSe}$ ,<sup>22</sup> relies on the formation of chainlike aggregates due to an induced dipole–dipole interaction. According to this synthetic scheme, each MnO would have six equivalent facets, and NC oligomers would assemble along the six directions of space. The reaction would terminate with an overgrowth of the chain end to form an arrow.

Hence, we believe that this quite unusual shape has resulted from a two-step mechanism. The growth seemed to involve the nucleation of truncated octahedra or cubes and, in a second step, the growth of homogeneous pods. Overall size and arm lengths are probably controlled by the precipitation of the multipods. Indeed, by decreasing the reaction time to 30 min overall, the particles adopt

a truncated octahedra shape. Particle size around 40–50 nm was in good agreement with chain end diameter, and some particles coalesced to form aggregates, as shown in Figure 3. The structure was also manganosite as confirmed by ED.

In conclusion, we have prepared high quality single-crystalline MnO multipods. This simple procedure offers new opportunities for the shape control of transition metal oxide. We are currently investigating the extension of this study to the other manganese oxides.

**Acknowledgment.** We thank Dr. Peter Werner from the Max-Planck-Institute of Microstructure Physics for assistance with the JEOL 4010 electron microscope.

**Supporting Information Available:** X-ray powder diffraction pattern and magnetic measurements of the MnO multipods. This material is available free of charge via the Internet at <http://pubs.acs.org>.

## References

- (1) Burda, C.; Chen, X.; Narayanan, R.; El-Sayed, M. A. *Chem. Rev.* **2005**, *105*, 1025.
- (2) Peng, X.; Manna, L.; Yang, W.; Wickham, J.; Scher, E.; Kadavanich, A.; Alivisatos, A. P. *Nature* **2000**, *404*, 59.
- (3) (a) Manna, L.; Scher, E. C.; Alivisatos, A. P. *J. Am. Chem. Soc.* **2000**, *122*, 12700. (b) Jun, Y.; Jung, Y.; Cheon, J. *J. Am. Chem. Soc.* **2002**, *124*, 615.
- (4) (a) Pinna, N.; Weiss, K.; Urban, J.; Pileni, M.-P. *Adv. Mater.* **2001**, *13*, 261. (b) Maillard, M.; Giorgio, S.; Pileni, M.-P. *Adv. Mater.* **2002**, *14*, 1084. (c) Jin, R.; Cao, Y. C.; Mirkin, C. A.; Kelly, K. L.; Schatz, G. C.; Zheng, J. G. *Science* **2001**, *294*, 1901.
- (5) Dumestre, F.; Chaudret, B.; Amiens, C.; Renaud, P.; Fejes, P. *Science* **2004**, *303*, 821.
- (6) (a) Ahmadi, T. S.; Wang, Z. L.; Green, T. C.; Henglein, A.; El-Sayed, M. A. *Science* **1996**, *272*, 1924. (b) Sun, Y. G.; Xia, Y. N. *Science* **2002**, *298*, 2176.
- (7) Yan, H.; He, R.; Pham, J.; Yang, P. *Adv. Mater.* **2003**, *15*, 402.
- (8) Johnson, C. J.; Dujardin, E.; Davis, S. A.; Murphy, C. J.; Mann, S. J. *Mater. Chem.* **2002**, *12*, 1765.
- (9) Kim, F.; Connor, S.; Song, H.; Kuykendall, T.; Yang, P. *Angew. Chem., Int. Ed.* **2004**, *43*, 3673.
- (10) Teng, X.; Yang, H. *Nano Lett.* **2005**, *5*, 885.
- (11) Rao, C. N. R.; Raveau, B. *Transition Metal Oxides*; VCH Publishers: New York, 1995.
- (12) (a) Solovoyev, I. V.; Terakura, K. *Phys. Rev. B* **1998**, *58*, 15496. (b) Nayak, S. K.; Jena, P. *J. Am. Chem. Soc.* **1999**, *121*, 644.
- (13) (a) Hyeon, T. *Chem. Commun.* **2003**, 927. (b) Tang, J.; Fabbri, J.; Robinson, R. D.; Zhu, Y. M.; Herman, I. P.; Steigerwald, M. L.; Brus, L. E. *Chem. Mater.* **2004**, *16*, 1336. (c) Sun, S.; Zeng, H. *J. Am. Chem. Soc.* **2002**, *124*, 8204. (d) Pinna, N.; Neri, G.; Antonietti, M.; Niederberger, M. *Angew. Chem., Int. Ed.* **2004**, *43*, 4345. (e) Pinna, N.; Garnweitner, G.; Antonietti, M.; Niederberger, M. *J. Am. Chem. Soc.* **2005**, *127*, 5608.
- (14) Peng, X. *Chem.—Eur. J.* **2002**, *8*, 334.
- (15) Yin, M.; O'Brien, S. *J. Am. Chem. Soc.* **2003**, *125*, 10180.
- (16) Park, J.; An, K.; Hwang, Y.; Park, J.; Noh, H.; Kim, J.; Park, J.; Hwang, N.; Hyeon, T. *Nat. Mater.* **2004**, *3*, 891.
- (17) Seo, W. S.; Jo, H. H.; Lee, K.; Kim, B.; Oh, S. J.; Park, J. T. *Angew. Chem., Int. Ed.* **2004**, *43*, 1115.
- (18) (a) Nayak, S. K.; Jena, P. *Phys. Rev. Lett.* **1998**, *81*, 2970. (b) Pask, J. E.; Singh, D. J.; Mazin, I. I.; Hellberg, C. S.; Kortus, J. *Phys. Rev. B* **2001**, *64*, 024403.
- (19) (a) Penn, R. L.; Banfield, J. F. *Science* **1998**, *281*, 969. (b) Polleux, J.; Pinna, N.; Antonietti, M.; Niederberger, M. *Adv. Mater.* **2004**, *16*, 436.
- (20) Pacholski, C.; Kornowski, A.; Weller, H. *Angew. Chem., Int. Ed.* **2002**, *41*, 1188.
- (21) Tang, Z.; Kotov, N. A.; Giersig, M. *Science* **2002**, *297*, 237.
- (22) (a) Lifshitz, E.; Bashouti, M.; Kloper, V.; Kigel, A.; Eisen, M. S.; Berger, S. *Nano Lett.* **2003**, *3*, 857. (b) Cho, K.; Talapin, D. V.; Gaschler, W.; Murray, C. B. *J. Am. Chem. Soc.* **2005**, *127*, 7140.

JA0555926